Journal of Theoretical and Applied Information Technology
20th December 2014. Vol.70 No.2

ISSN: 1992-8645 www.jatit.org E-ISSN: 1817-3195

IMPACT OF THE STATOR RESISTANCE OF SQUIRREL CAGE INDUCTION MOTOR USING DIRECT TORQUE CONTROL AND PI CONTROLLER

[1]RIDWAN GUNAWAN, [2]FERI YUSIVAR
[1,2]Department of Electrical Engineering, Universitas Indonesia, Depok, Indonesia.
Email: [1]ridwan@eng.ui.ac.id , [2]yusivar@ieee.org

ABSTRACT

The three-phase induction motor squirrel cage has a characteristic change in the event of a change in temperature beyond the motor operation, which leads to changes in the stator so that the resistance value affects the performance of the rotational speed of the motor, the motor rotation speed changes are influenced by the amount flux generated by the flow of resistance in stator. This paper aims to monitoring the motor rotation speed a characteristic three phase squirrel cage induction againts shift in the stator resistance value using a PI controller and a sensor of the motor speed in which the reference modeling is used motor stator current and stator flux. All of the three phase system is transformed in quadrature and direct axis.The resistance change of approach to equality of the number of turns in each phase in the stator. The Direct Torque Control method is used because the process of the motor speed is determined by the stator flux, torque, and position the sector to determine the input of inverter switching obtained from the Lookup Table [6]. The value of resistance in flux estimation gives the value of the flux hysteresis band against the actual performance.

Keywords: *Stator resistance, Three-phase Induction motor Squirrel Cage, Direct Torque Control (DTC), Proportional and Integral controller (PI Controller) , Quadrature-Direct axis (qd-axis)*

1. INTRODUCTION

The production machines in the various industries , many to use induction motor as a primemover. The stator short circuit fault in the industrial induction motor is the faults typically have a significant share of about 38% amongst the common type of faults in industrial induction motors. Therefore, it is very important to detect such faults.

The circulating current will increase when the stator winding inter-turn short circuit fault or the air-gap eccentricity fault occurs. A method of induction machine fault diagnosis, based on the stator winding parallel-connected branches circulating current characteristics[1]. Through calculating the machine parameters of air-gap magnetomotive force, air-gap magnetic field energy and magnetic flux density on the fault, the frequency characteristic of imbalance magnetic pull acting on rotor and that of pulsating magnetic pull acting on stator core are found out[2]. Using the stator winding as the fault detection winding, the corresponding relationships between the faults levels of rotor winding inter turn short-circuit and the effective magnetic field loss is established [3]. The major drawbacks of model-based techniques are the requirements of precise motor parameters and the need of speed signals in addition to the voltage and current. The induction motor model that is developed is independent of rotor speed in and, thus, the diagnostic method is also independent of the torque variation [4].

The effect of damper winding configuration on unbalanced magnetic pull, was performed, that damper winding resistivity and the distance between the damper bars in a pole determine the effectiveness of the damper winding in reducing the unbalanced magnetic pull,. that the reduction can be substantial from damper windings with low resistivity[5]. The dependence on the parameter of machines, a method to extract the component produced by the fault from the estimation error is presented in [10].

The stator winding faults create unbalancing in the line current, and similar unbalancing is also

Journal of Theoretical and Applied Information Technology
20th December 2014. Vol.70 No.2

ISSN: 1992-8645 www.jatit.org E-ISSN: 1817-3195

created due to asymmetrical winding resistances, the circuit connection resistances and supply unbalance.[11,12].

Shorted turns in stator windings often do not affect the normal operation in the early stage. However, eventually that can grow into serious motor failure. Majority of motor stator winding failure happens due to the destruction of the turn insulation caused by the short circuit in stator windings [8][9]. One of the problem is the influence of inductances between phases, and other problems , unbalance of the input voltage and the influence of stator temperature , so that the rotor speed characteristic becomes unstable.

The speed error occur cause change the stator magnetic flux, that some of stator conductors have short circuit condition, and this condition is called inter turn short circuit and the motor temperature rise[6], so that cause the stator resistance change its value. The Direct Torque Control is used as a control system of the induction motor using voltage source is an inverter [7]. This method makes possible do to direct controlled the torque and flux of the induction motor using to select voltage vector . The choice voltage vector limited torque and flux in the hysteris band and reach torque response very short time.

The modeling of induction motor with some of conductor in each phase stator will be used , for obtain torque, flux, current and input voltage performance using DTC , this matter cause the influence of stator as the flux is generated .

In this paper is designed a speed controller using sensor dan PI controller, for three phase induction motor squirrel cage, so that the speed response performance motor, can be reach, when the resistance of stator change , cause short circuit at some stator

2 METHODOLOGY

The motor model is three phase , squirrel cage using change resistance is modeled with amount of stator conductors each phase. The turns of each phase is used amount of turns at three conditions are 252, 222 and 200 turns. .

The motor model is dynamic, using stator reference , 2 HP, 380 volt, 60 Hz and 4 pole. The control method is used DTC using PI controller and speed sensor ,

Kp= 0.00316 and Ki= 0.089. The motor parameter is counted using M-File and Matlab Simulink version 7.6.0.3.2.4A.

2.1 Modeling Induction Motor in qd axis

Induction motor model that used is a three phase motor model. In case to make estimation and analysis easier, there's a need to transform three phase model of induction motor such as current, voltage, and flux into two phase model. The Clarke and Park Transformation is used for transformation of three phase model to stationary axis two phase model alfa-beta and then to transform the stationary axis two phase model to rotating axis of two phase model qd axis. The motor model in qd axis reference base on stator reference with model parameters are stator current and flux, that the value of stator synchrone speed ω = 0, is obtained the equation for qd-axis as follows : [5]

$$\frac{d}{dt}i_q^s = \frac{\frac{r^r}{L_{12}^{sr}}}{\left(\frac{L_{22}^{rr}L_{11}^{ss}}{L_{12}^{sr}} - L_{21}^{sr}\right)}\lambda_q^s - \frac{\left(\frac{r^r L_{11}^{ss}}{L_{12}^{sr}} + \frac{r_{11}^s L_{22}^{rr}}{L_{12}^{sr}}\right)}{\left(\frac{L_{22}^{rr}L_{11}^{ss}}{L_{12}^{sr}} - L_{21}^{sr}\right)}i_q^s + \frac{\frac{L_{22}^{rr}}{L_{12}^{sr}}}{\left(\frac{L_{22}^{rr}L_{11}^{ss}}{L_{12}^{sr}} - L_{21}^{sr}\right)}V_q^s - \frac{\left(\frac{L_{11}^{rr}L_{22}^{ss}}{L_{21}^{sr}} - L_{12}^{sr}\right)}{\left(\frac{L_{22}^{rr}L_{11}^{ss}}{L_{12}^{sr}} - L_{21}^{sr}\right)}\omega_r i_d^s - \frac{\frac{L_{11}^{rr}}{L_{21}^{sr}}}{\left(\frac{L_{22}^{rr}L_{11}^{ss}}{L_{12}^{sr}} - L_{21}^{sr}\right)}\omega_r \lambda_d^s \qquad (1)$$

$$\frac{d}{dt}i_d^s = \frac{\frac{r^r}{L_{21}^{sr}}}{\left(\frac{L_{11}^{rr}L_{22}^{ss}}{L_{21}^{sr}} - L_{12}^{sr}\right)}\lambda_d^s - \frac{\left(r^r\frac{L_{22}^{ss}}{L_{21}^{sr}} + r_{22}^s\frac{L_{11}^{rr}}{L_{21}^{sr}}\right)}{\left(\frac{L_{11}^{rr}L_{22}^{ss}}{L_{21}^{sr}} - L_{12}^{sr}\right)}i_d^s + \frac{\frac{L_{11}^{rr}}{L_{21}^{sr}}}{\left(\frac{L_{11}^{rr}L_{22}^{ss}}{L_{21}^{sr}} - L_{12}^{sr}\right)}V_d^s - \frac{\left(\frac{L_{22}^{rr}L_{11}^{ss}}{L_{12}^{sr}} - L_{21}^{sr}\right)}{\left(\frac{L_{11}^{rr}L_{22}^{ss}}{L_{21}^{sr}} - L_{12}^{sr}\right)}\omega_r i_q^s - \frac{\frac{L_{22}^{rr}}{L_{12}^{sr}}}{\left(\frac{L_{11}^{rr}L_{22}^{ss}}{L_{21}^{sr}} - L_{12}^{sr}\right)}\omega_r \lambda_q^s \qquad (2)$$

$$\frac{d}{dt}\lambda_q^s = -r_{11}^s i_q^s + V_q^s \qquad (3)$$

$$\frac{d}{dt}\lambda_d^s = -r_{22}^s i_d^s + V_d^s \qquad (4)$$

Journal of Theoretical and Applied Information Technology
20th December 2014. Vol.70 No.2

ISSN: 1992-8645 www.jatit.org E-ISSN: 1817-3195

2.2 Modeling of Amount Stator Turns in qd axis

The equations of induction motor circuit can be written in vector system. A symmetrical model induction motor, three phase can obtain from vector space motor at rotor speed cause of flux link from stator [1]. The stator and rotor equations when the turns flux unbalance condition can be written as below :

$$V_{abc}^{s} = r_{abc}^{s} i_{abc}^{s} + \dot{\lambda}_{abc}^{s} \quad (5)$$

$$0 = r_{abc}^{r} i_{abc}^{r} + \dot{\lambda}_{abc}^{r} \quad (6)$$

The model of stator turns are equivalent circuit of resistance and inductance with series conection, in the three phase system is shown as figure 1.

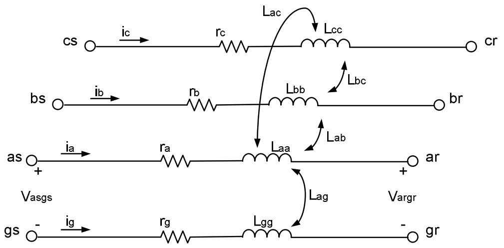

Figure 1: Three phase resistance-inductance series

The stator voltage and flux equations : $V_s =$

$$\begin{bmatrix} R_a & 0 & 0 \\ 0 & R_b & 0 \\ 0 & 0 & R_c \end{bmatrix} i_s + \begin{bmatrix} \frac{d\Lambda_{sa}}{dt} \\ \frac{d\Lambda_{sb}}{dt} \\ \frac{d\Lambda_{sc}}{dt} \end{bmatrix} \quad (7)$$

$$\Lambda_s = \mathbf{L}_{abc}^{ss} i_s + \begin{bmatrix} L_{asr} \\ L_{bsr} \\ L_{csr} \end{bmatrix} i_r \quad (8)$$

The element matrices r_{qd}^{s} motor model is obtained from relationship resistance between phases a,b and c , and then is trasformed to resistance in q and d axis .

$$r_{qd}^{s} = \begin{bmatrix} r_{11}^{s} & r_{12}^{s} & r_{13}^{s} \\ r_{21}^{s} & r_{22}^{s} & r_{23}^{s} \\ r_{31}^{s} & r_{32}^{s} & r_{33}^{s} \end{bmatrix} \begin{bmatrix} i_q^{s} \\ i_d^{s} \\ 0 \end{bmatrix} \quad (9)$$

Where

$$r_{11}^{s} = \frac{2}{3}\left(r_{as} + \frac{1}{4} r_{bs} + \frac{1}{4} r_{cs}\right) \quad (10)$$

$$r_{12}^{s} = \frac{\sqrt{3}}{6}(r_{bs} - r_{cs}) \quad (11)$$

$$r_{13}^{s} = \frac{1}{3}(2r_{as} - r_{bs} - r_{cs}) \quad (12)$$

$$r_{22}^{s} = \frac{1}{2}(r_{bs} + r_{cs}) \quad (13)$$

$$r_{33}^{s} = \frac{1}{3}(2r_{as} + r_{bs} + r_{cs}) \quad (14)$$

$$r_{21}^{s} = r_{12}^{s},\ r_{23}^{s} = -\frac{1}{2} r_{12}^{s} \quad (15)$$

$$r_{31}^{s} = -\frac{1}{2} r_{12}^{s} \ \text{ and } \ r_{32}^{s} = -r_{12}^{s} \quad (16)$$

Where :

$$r_{as} = \frac{N_a}{N_s} r_s,\ r_{bs} = \frac{N_b}{N_s} r_s,\ r_{cs} = \frac{N_c}{N_s} r_s \ \text{ and}$$

$$N_a = N_b = N_c = N_s \quad (17)$$

$$r_{dq0}^{r} = r_r \mathbf{I}_{3\times3} \quad (18)$$

Na,Nb and Nc are total amount of phase turns at phase a, b and c.

The stator and rotor turns flux are written as below :

$$\begin{bmatrix} \lambda_{abc}^{s} \\ \lambda_{abc}^{r} \end{bmatrix} = \begin{bmatrix} \mathbf{L}_{abc}^{ss} & \mathbf{L}_{abc}^{sr} \\ \mathbf{L}_{abc}^{rs} & \mathbf{L}_{abc}^{rr} \end{bmatrix} \begin{bmatrix} \mathbf{i}_{abc}^{s} \\ \mathbf{i}_{abc}^{r} \end{bmatrix} \quad (19)$$

the stator and rotor inductance

$$\mathbf{L}_{abc}^{ss} = \begin{bmatrix} L_{asas} & L_{asbs} & L_{ascs} \\ L_{bsas} & L_{bsbs} & L_{bscs} \\ L_{csas} & L_{csbs} & L_{cscs} \end{bmatrix} \quad (20)$$

$$\mathbf{L}_{abc}^{rr} = \begin{bmatrix} L_{arar} & L_{arbr} & L_{arcr} \\ L_{brar} & L_{brbr} & L_{brcr} \\ L_{crar} & L_{crbr} & L_{crcr} \end{bmatrix} \quad (21)$$

Using symmetrically principle and relationship between inductors stator and rotor , is obtained the inductance equation between stator and rotor in the rotor angle is shown below, [2]

$$\mathbf{L}_{abc}^{sr} = \begin{bmatrix} L_{asar}\cos\theta_r & L_{asbr}\cos\left(\theta_r + \frac{2\pi}{3}\right) & L_{ascr}\cos\left(\theta_r - \frac{2\pi}{3}\right) \\ L_{bsar}\cos\left(\theta_r - \frac{2\pi}{3}\right) & L_{bsbr}\cos\theta_r & L_{bscr}\cos\left(\theta_r + \frac{2\pi}{3}\right) \\ L_{csar}\cos\left(\theta_r + \frac{2\pi}{3}\right) & L_{csbr}\cos\left(\theta_r - \frac{2\pi}{3}\right) & L_{cscr}\cos\theta_r \end{bmatrix} \quad (22)$$

Using symmetrically principle between stator and rotor, then $L_{asar} = L_{asbr} = L_{ascr}$,

$$L_{bsar} = L_{bsbr} = L_{bscr}$$

$$L_{csar} = L_{csbr} = L_{cscr}. \quad (23)$$

The equation flux line stator and rotor in $qd0$ axis is obtained from the Clark and Park transformation, equation (7).

$$\lambda_{qd0}^{s} = \mathbf{L}_{qd0}^{ss} \mathbf{i}_{qd0}^{s} + \mathbf{L}_{qd0}^{sr} \mathbf{i}_{qd0}^{r} \quad (24)$$

$$\lambda_{qd0}^{r} = \mathbf{L}_{qd0}^{rs} \mathbf{i}_{qd0}^{s} + \mathbf{L}_{qd0}^{rr} \mathbf{i}_{qd0}^{r} \quad (25)$$

Where :

$$\mathbf{L}_{qd0}^{ss} = \begin{bmatrix} L_{11}^{ss} & L_{12}^{ss} & L_{13}^{ss} \\ L_{21}^{ss} & L_{22}^{ss} & L_{23}^{ss} \\ L_{31}^{ss} & L_{32}^{ss} & L_{33}^{ss} \end{bmatrix} \quad (26)$$

$$\mathbf{L}_{qd0}^{sr} = \begin{bmatrix} L_{11}^{sr} & L_{12}^{sr} & 0 \\ L_{21}^{sr} & L_{22}^{sr} & 0 \\ L_{31}^{sr} & L_{32}^{sr} & 0 \end{bmatrix} \quad (27)$$

$$\mathbf{L}_{qd0}^{rr} = \begin{bmatrix} L_{11}^{rr} & 0 & 0 \\ 0 & L_{22}^{rr} & 0 \\ 0 & 0 & L_{33}^{rr} \end{bmatrix} \quad (28)$$

$$\mathbf{L}_{qd0}^{rs} = \begin{bmatrix} L_{11}^{sr} & L_{12}^{sr} & 0.5L_{13}^{sr} \\ L_{21}^{sr} & L_{22}^{sr} & -0.5L_{32}^{sr} \\ 0 & 0 & 0 \end{bmatrix} \quad (29)$$

The element of matrices $\mathbf{L}_{qd0}^{ss}, \mathbf{L}_{qd0}^{sr}, \mathbf{L}_{qd0}^{rr}, \mathbf{L}_{qd0}^{rs}$ consist of :

Journal of Theoretical and Applied Information Technology
20th December 2014. Vol.70 No.2

ISSN: 1992-8645 www.jatit.org E-ISSN: 1817-3195

The qd0 stator and mutual inductance, element of L_{qd0}^{ss}

$$L_{11}^{ss} = \frac{2}{3}(L_{asas} + .25L_{bsbs} + .25L_{cscs} - L_{asbs} - L_{ascs} - .5L_{bscs}) \quad (30)$$

$$L_{12}^{ss} = \frac{1}{2\sqrt{3}}(L_{bsbs} - L_{cscs} + L_{ascs}) \quad (31)$$

$$L_{13}^{ss} = \frac{2}{3}(L_{asas} - .5L_{bsbs} - .5L_{cscs} + .5L_{asbs} + .5L_{ascs} - L_{bscs}) \quad (32)$$

$$L_{21}^{ss} = \frac{1}{\sqrt{3}}(.5L_{bsbs} - .5L_{cscs} - L_{asbs} + L_{ascs}) \quad (33)$$

$$L_{22}^{ss} = \frac{1}{2}(L_{bsbs} + L_{cscs} - 2L_{bscs}) \quad (34)$$

$$L_{23}^{ss} = \frac{1}{\sqrt{3}}(-L_{bsbs} + L_{cscs} - L_{asbs} + L_{ascs}) \quad (35)$$

$$L_{33}^{ss} = \frac{1}{3}(L_{asas} + L_{bsbs} + L_{cscs} + 2L_{asbs} + 2L_{ascs} + 2L_{bscs}) \quad (36)$$

$$L_{31}^{ss} = \frac{1}{2}L_{13}^{ss} \qquad L_{32}^{ss} = \frac{1}{2}L_{23}^{ss} \quad (37)$$

where

$$L_a = L_b = L_c, L_{asas} = L_{bsbs} = L_{cscs}$$
$$L_{asbs} = L_{ascs} = L_{bscs} \quad (38)$$

The *qd0* stator to rotor and mutual inductance, Element of L_{qd0}^{sr}

Cause the rotor symmetric, that the coefficient of relationship stator to rotor inductance can be simpled using this form below .

$$L_{asar} = L_{asbr} = L_{ascr} = L_{asr},$$
$$L_{bsar} = L_{bsbr} = L_{bscr} = L_{bsr},$$
$$L_{csar} = L_{csbr} = L_{cscr} = L_{csr}, \quad (39)$$

$$L_{11}^{sr} = L_{asr} + .25L_{bsr} + .25L_{csr} \quad (40)$$

$$L_{12}^{sr} = \frac{\sqrt{3}}{4}(L_{bsr} - L_{csr}) \quad (41)$$

$$L_{22}^{sr} = \frac{3}{4}(L_{bsr} + L_{csr}) \quad (42)$$

$$L_{31}^{sr} = .5L_{asr} - .25L_{bsr} - .25L_{csr} \quad (43)$$

$$L_{21}^{sr} = L_{12}^{sr}, \text{ and } L_{32}^{sr} = -L_{12}^{sr}. \quad (44)$$

The qd0 rotor and inductance conection.

$$L_{11}^{rr} = L_{22}^{rr} = L_{lr} + \frac{3}{2}L_{mar} = L_{lr} + \frac{N_r^2}{N_s^2}L_m \quad (45)$$

$$L_{33}^{rr} = L_{lr} \quad (46)$$

The flux stator and rotor in qd0 axis system is written as below :

$$\begin{bmatrix} \lambda_q^s \\ \lambda_d^s \\ \lambda_q^r \\ \lambda_d^r \end{bmatrix} = \begin{bmatrix} L_{11}^{ss} & L_{12}^{ss} & L_{11}^{sr} & L_{12}^{sr} \\ L_{21}^{ss} & L_{22}^{ss} & L_{21}^{sr} & L_{22}^{sr} \\ L_{11}^{sr} & L_{12}^{sr} & L_{11}^{rr} & 0 \\ L_{21}^{sr} & L_{22}^{sr} & 0 & L_{22}^{rr} \end{bmatrix} \begin{bmatrix} i_q^s \\ i_d^s \\ i_q^r \\ i_d^r \end{bmatrix} \quad (47)$$

Tthe stator inductance is written

$$L_{asas} = \frac{N_a^2}{N_s^2}\left(L_{ls} + \frac{2}{3}L_m\right) = N_a^2 L_{mls} \quad (48)$$

$$L_{bsbs} = N_b^2 L_{mls} \quad (49)$$

$$L_{cscs} = N_c^2 L_{mls} \quad (50)$$

Where

$$L_{mls} = \frac{1}{N_s^2}\left(L_{ls} + \frac{2}{3}L_m\right) \quad (51)$$

N_a, N_b, N_c : total amount rotations of phase stator turn as, bs cs.

N_s: total amount of rotations turns reference.

And the stator induction between phase as-bs, bs-cs and cs-as can be controlled .

$$L_{asbs} = L_{bsas} = \left(-\frac{1}{2}N_a N_b\right)\left(\frac{2}{3}\frac{L_m}{N_s^2}\right) = -\frac{1}{3}\frac{N_a \quad N_b}{N_s^2}L_m = N_a N_b L_{mss} \quad (52)$$

$$L_{ascs} = L_{csas} = N_a N_c L_{mss} \quad (53)$$

$$L_{bscs} = L_{csbs} = N_b N_c L_{mss} \quad (54)$$

Where :

$$L_{mss} = -\frac{1}{3}\frac{L_m}{N_s^2} \quad (55)$$

The total rotor inductance is obtained at each phase ar,br,cr

$$L_{arar} = L_{brbr} = L_{crcr} =$$
$$L_{llr} + \frac{2}{3}\frac{N_r^2}{N_s^2}L_m = L_{lr} + L_{mar} \quad (56)$$

$$L_{mar} = \frac{2}{3}\frac{N_r^2}{N_s^2}L_m \quad (57)$$

The rotor mutual inductance ,

$$L_{arbr} = L_{arcr} = L_{brar} = L_{crar} = L_{crbr}$$
$$= -\left(\frac{1}{2}\right)\left(\frac{2}{3}\frac{N_r^2}{N_s^2}L_m\right) = -\frac{1}{2}L_{mar} \quad (58)$$

$N_{ar}, N_{br}, N_{cr} = N_r$: total amount rotations of phase rotor turns ar, br, cr

$$L_{asar} = L_{asbr} = L_{ascr} = \frac{2}{3}\frac{N_a \quad N_r}{N_s^2}L_m = N_a L_{msr}. \quad (59)$$

$$L_{bsar} = L_{bsbr} = L_{bscr} = \frac{2}{3}\frac{N_b \quad N_r}{N_s^2}L_m = N_b L_{msr} \quad (60)$$

$$L_{csar} = L_{csbr} = L_{cscr} = \frac{2}{3}\frac{N_c \quad N_r}{N_s^2}Lm = N_c \quad (61)$$

Where :

$$L_{msr} = \frac{2}{3}\frac{N_r}{N_s^2}L_m \quad (62)$$

2.3 Modeling of Induction Motor using Direct Torque Control

The Direct Torque Control is a method torque controlled direct using electromagnetic torque motor *Te*. In DTC system can be done the direct torque controlled and stator flux using the choice of voltage vector (selector voltage). DTC Block diagram consist of hystheresis comparator, torque estimator, flux magnitude value, flux position calculation and voltage selector as input the inverter

Journal of Theoretical and Applied Information Technology
20th December 2014. Vol.70 No.2

ISSN: 1992-8645 www.jatit.org E-ISSN: 1817-3195

source , (Voltage Source Inverter).The hystheresis torque *level three* and the hystheresis flux *level two* is used , and the output of its, both as input to look-up table, for the choice voltage vector in Look Up table as inverter input voltage. The Look Up table has six voltage vector and two voltage vector Null (0) as the output inverter, that is V0, V1, V2, V3, V4, V5, V6, and V7. [6],[10]

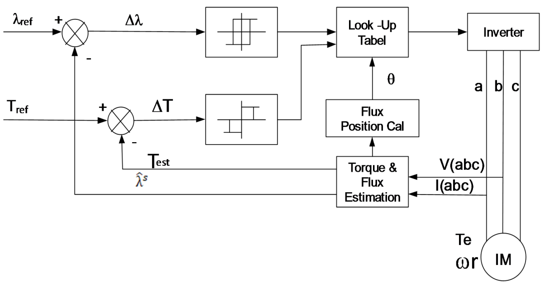

Figure 2: Direct Torque Control Block Diagram

Tabel 1: The choice voltage vector at each sector.

φ	Te	Sector					
		1	2	3	4	5	6
cφ=1	CT=1	V2	V3	V4	V5	V6	V1
	CT=0	V7	V0	V7	V0	V7	V0
	CT= -1	V6	V1	V2	V3	V4	V5
cφ= -1	CT=1	V3	V4	V5	V6	V1	V2
	CT=0	V0	V7	V0	V7	V0	V7
	CT= -1	V5	V6	V1	V2	V3	V4

The flux condition : If cφ = 1 , the flux must be risen and if cφ = -1 , the flux must be reduced. For Torque condition : cT =1 means the torque must be risen , and at cT = 0 , the torque value still at this position. And at cT = -1, the torque must be reduced.

The estimate process using a voltage model, the estimate parameter is obtained using stator flux estimate equations. The stator flux and torque estimate are counted using these equations below :

$$\lambda_q^s = \int (v_q^s - r_s i_q^s) dt \quad (63)$$

$$\lambda_d^s = \int (v_d^s - r_s i_d^s) dt \quad (64)$$

$$v_q^s = \frac{2}{3}\left[v_{as} - \frac{1}{2}(v_{bs} + v_{cs})\right] \quad (65)$$

$$v_d^s = \frac{1}{\sqrt{3}}[-v_{bs} + v_{cs}] \quad (66)$$

The stator flux estimate using amount of turns is written as below :

$$v_d^s = \frac{1}{\sqrt{3}}[-v_{bs} + v_{cs}] \quad (67)$$

$$\hat{\lambda}_d^s = \int \left(v_d^s - r_{21}^s i_q^s - r_{22}^s i_d^s\right) dt \quad (68)$$

$$\hat{\lambda}^s = \sqrt{\left(\hat{\lambda}_q^s\right)^2 + \left(\hat{\lambda}_d^s\right)^2} \quad (69)$$

The torque equation is written as :

$$T_e = \frac{3}{2}\frac{P}{2}\left(\hat{\lambda}_d^s i_q^s - \hat{\lambda}_q^s i_d^s\right) \quad (70)$$

And the flux stator position is written as :

$$\hat{\theta}_{fluks} = \tan^{-1}\left(\frac{\hat{\lambda}_q^s}{\hat{\lambda}_d^s}\right) \quad (71)$$

3 DISCUSSION

The block diagram system using the squirrel cage induction motor 2 horsepower, three phase, 60 hertz and 380 volt is shown as figure 3.

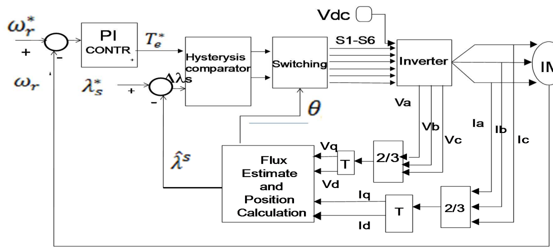

Figure 3: Direct Torque Control Block Diagram

This simulation will show, rotor speed (ω_r), stator flux (λ_s) and the current at a single phase in d axis (i_d). Torque hystheresis constant 0.06, (maximum value 6) and the flux hystheresis constant 0.12 , proportional constant Kp = 0.00316, integral constant Ki = 0.089.

Tabel 2: The motor parameter 2 horsepower [7]

no	Motor Power		2	HP
1	total of pole	p	4	-
2	Stator resistance	Rs	4.05	Ohm
3	Rotor resistance	Rr	2.60	Ohm
4	Stator Inductance	Ls	0.01397	henry
5	Rotor Inductance	Lr	0.01397	henry
6	Mutual Inductance	L_m	0.53868	henry
7	Moment of Inertia	J	0.06	Kgm^2
8	Damping coeff.	D	0.089	Ns/m
9	Tot amount o turns	N	252	trn/ph

$r_{11}^s = r_{21}^s = 1.35$ ohm,
$r_{12}^s = r_{22}^s = 0$

These simulations will be done at no load, using amount of :

1. Symmetrical Turns Each Phase.
   Simulation using amount of symmetrical turns each phase at is 252 turn.
2. Unsymmetrical Turns at phase B-222 turns and phase A and C-252 turns.
3. Unsymmetrical Turns at phase B-200 turns and phase A and C-252 turns.

Journal of Theoretical and Applied Information Technology
20th December 2014. Vol.70 No.2

ISSN: 1992-8645 www.jatit.org E-ISSN: 1817-3195

The results from these simulations are the rotor speed (ω_r), currents : phase a (I_a^s), phase b (I_b^s), stator flux (λ_s), torque (T_e) and input stator voltage at d axis, (v_{ds}). [4]

3.1 Simulation Rotor Speed Using Amount of Symmetrical And Unsymmetrical Turns

3.1.1 Simulation Using Amount of Symmetrical Turns Each Phase.

The turns at each phase is 252 turn.

The DTC method using PI controller, gives response to change the refrence value, what it is shown as figure 4 .

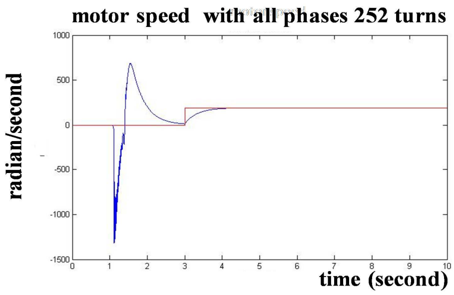

Figure 4: rotor speed with Amount of Symmetrical Turns Each Phase is 252 turns at No Load

The rotor speed signal responsed at time 0.54 second and at time 1.56 seconds the rotor speed overshoot until 750 radian/second and at time 3 seconds the rotor speed can follow the reference control signal.

3.1.2 Simulation Using Amount of Unsymmetrical Turns at Phase B .

In this simulation the amount of turns in each phase is symmetric at time t = 0 (start condition),until time 6 seconds, and after t = 6 seconds the amount of turns in phase B, not symmetric with other phases. .

In this condition, at time 6 seconds after the turns at phase B decrease become 222 turns (short of turns) the rotor speed rise overshoot the reference speed along 0.8 seconds, the maximum overshoot reach 400 radians/second is shown as figure 5.

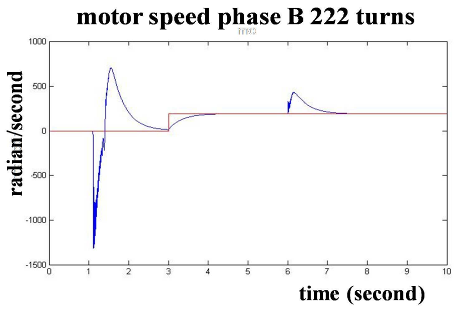

Figure 5: Rotor speed with Amount of Unsymmetrical Turns at Phase B is 222 turns at No Load.

In this condition, at time 6 seconds after the turns at phase B decrease to become 200 turns (short of turns) the rotor speed rise overshoot the reference speed along 1.3 seconds until time 7.3 seconds , the maximum overshoot reach 500 radians/second , is shown as figure 6

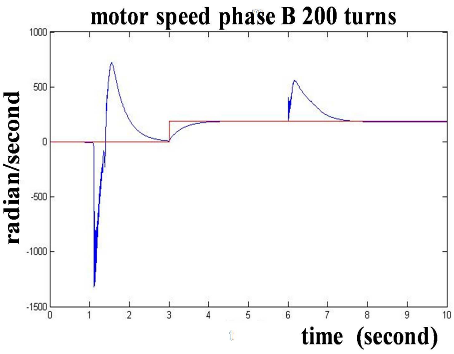

Figure 6 rotor speed with Amount of Unsymmetrical Turns at Phase B is 200 turns at No Load.

The rise in disturbance of the motor speed from figure 5 and figure 6 is compared with normal condition curve at figure 4 show, this conditions show , that it have a unbalancing asymetrical turn.

3.2 Simulation The Stator Current Using Amount of Symmetrical And Unsymmetrical Turns

3.2.1. The Stator Current Using Amount of Symmetrical Turns Each Phase.

The turns at each phase is 252 turn.

The current phasa A shows at time 0.54 seconds is 1.54 amperes, at time 3 seconds the current decrease 0.74 amperes and at time 3.3 seconds the current constant 4 amperes is shown as figure 7.

ISSN: 1992-8645 www.jatit.org E-ISSN: 1817-3195

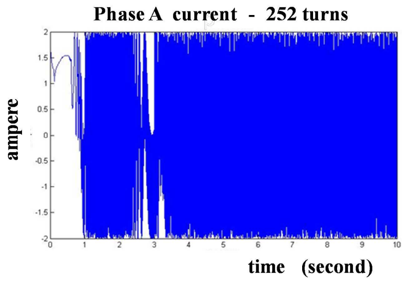

Figure 7: The Phase A Current - 252 turns

The current phasa B shows after time 4.8 seconds the average current is 1.4 amperes is shown as figure 8.

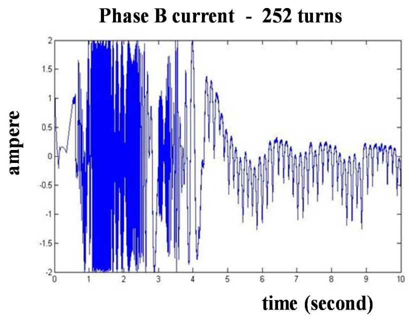

Figure 8: The Phase B Current-252 turns

3.2.2 The Stator Current Using Amount of Unsymmetrical Turns at Phase B .

The current phasa B shows at time 0.54 seconds is 1.7 amperes, after time 4.8 until 6 seconds the average current is 1.2 amperes, at time 6 seconds the current decreases along 1.2 seconds until time 7.2 seconds .In this condition, at time 6 seconds the current overshoot until 4 amperes an then decrease along 0.5 seconds and raise again until time 7.2 seconds , is shown as figure 9.

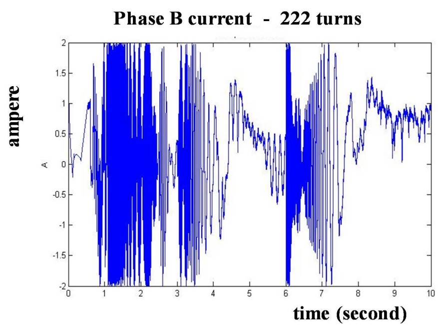

Figure 9: The Phase B Current-222 turns

The current phasa B shows at time 6 seconds the current overshoot until 4 amperes an then decrease along 0.5 seconds and raise again until time 7.2 seconds , is shown as figure 10.

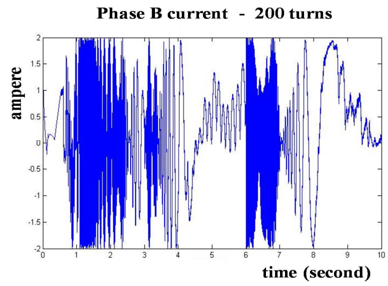

Figure 10: The Phase B Current -200 turns

The rise in disturbance of the motor current from figure 9 and figure 10 is compared with normal condition curve at figure 8 show, this conditions show , that it found the unbalancing motor current, in the line current phase, and this condition is also created due to asymmetrical winding resistances or it shows to indicate the short circuit at B phase .

3.3 Simulation The Stator Flux Using Amount of Symmetrical And Unsymmetrical Turns

3.3.1. The Stator Flux Using Amount of Symmetrical Turns Each Phase.

The turns at each phase is 252 turn.The flux response shows begin at time 0.54 seconds after the controller actives, the actual flux can follow the estimate flux , reach time one second, and between t=1 until 1.6 seconds the flux decrease 20.5 weber, and rise again until time 3.3seconds. the flux constant at position 35.6 weber is shown as figure 11.

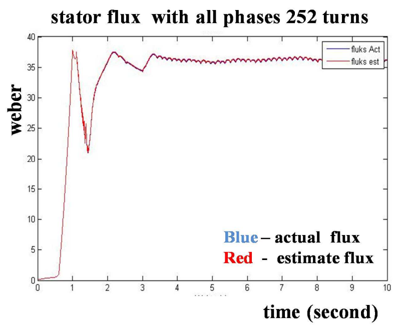

Figure11: The actual and estimate fluxs

3.3.2 The Stator Flux Using Amount of Unsymmetrical Turns at Phase B .

The flux response shows begin at time 0.54 detik after the controller actives, the actual flux can

Journal of Theoretical and Applied Information Technology
20th December 2014. Vol.70 No.2

ISSN: 1992-8645 www.jatit.org E-ISSN: 1817-3195

follow the estimate flux , reach time one and half second, and between t=1.5still the flux estimate can follow the flux actual but less then. At time 6 seconds, the flux decrease to reach 35 weber, is shown as figure 12.

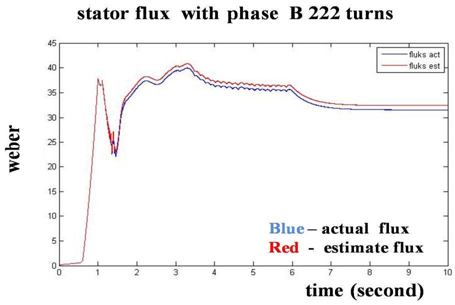

. *Figure 12: The actual and estimate fluxs-phase B 222 turns*

At time 6 seconds, the flux decrease to reach 35 weber, and after time 6 seconds the flux estimate can follow the flux actual , is shown as figure 13.

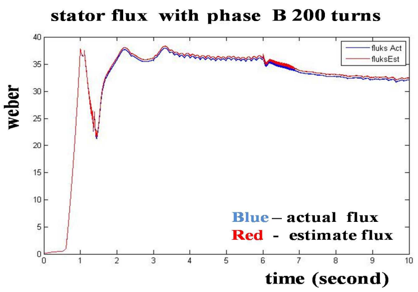

Figure 13: The actual and estimate fluxs phase B 200 turns

The decreasing disturbance of the stator flux in figure 12 and figure 13 shows, a presented the error of stator flux, if it is compared to the normal stator flux in figure 11, that it occure the short circuit turn-to turn at B phase.

3.4 Simulation The Electromagnetic Torque Using Amount of Symmetrical And Unsymmetrical Turns

3.4.1.The Electromagnetic Torque Using Amount of Symmetrical Turns Each Phase.

The turns at each phase is 252 turn.

The motor torque at time 0.54 second has value 0.12 Newton .meters, and at time 1.1 seconds rise reach 1.1x10e4 Newton.meters , at time 3 seconds the motor speed is controlled, the motor torque reach peak value 18 Newton.meters and stable at time 4.2 seconds with average torque value 0.9554 Newton.meters is shown as figure 14.

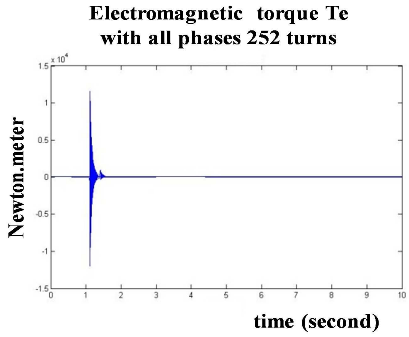

Figure 14: The Electromagnetic Torque motor

3.4.2 The Electromagnetic Torque Using Amount of Unsymmetrical Turns at Phase B .

The motor torque at time 0.54 second has value 0.12 Newton .meters, and at time 1.1 seconds rise reach 1.1x10e4 Newton.meters , at time 3 seconds the motor speed is controlled, the motor torque reach peak value 18Newton.meters and stable at time 4.2 seconds with average torque value 0.9554 Newton.meters , at time 6 seconds the torque overshoot along 0.1 seconds and the maximum overshoot value is 0.05x 10e4 Newton.meters, is shown as figure 15.

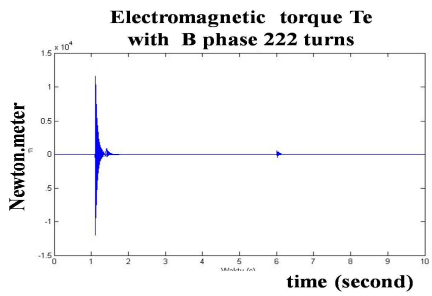

Figure 15: The Electromagnetic Torque motor-phase B 222 turns

In this condition, at time 6 seconds the torque overshoot along 0.1 seconds and the maximum overshoot value is 0.1x 10e4 Newton.meters, is shown as figure 19.is shown as figure 16

ISSN: 1992-8645 www.jatit.org E-ISSN: 1817-3195

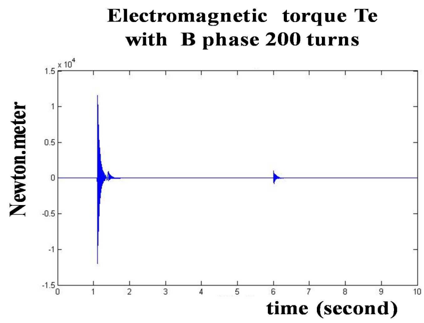

Figure 16: The Electromagnetic Torque motor-phase B 200 turns

The strong influence of the flux to the electromagnetic torque, shows the electromagnetic torque disturbance increase in figure 15 and figure 16 , is compared with normal condition curve at figure 14, show this indicate the short circuit at B phase.

3.5 Simulation The Inverter Voltage Using Amount of Symmetrical And Unsymmetrical Turns

3.5.1. The Inverter Voltage Using Amount of Symmetrical Turns Each Phase.

The turns at each phase is 252 turn. The inverter input voltage shows that the voltage choice from input signal *look up table* to inverter , at time 0.56 seconds, the choice process is good , is shown as figure 17.

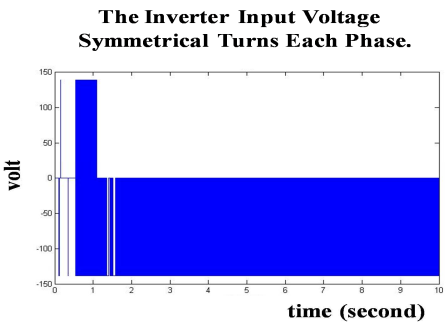

Figure 17: The input inverter voltage.

3.5.2 The Inverter Voltage Using Amount of Unsymmetrical Turns at Phase B .

The inverter input voltage shows that the voltage choice from input signal *look up table* to inverter , at time 0.56 seconds, the choice process is still good , is shown as figure 18.

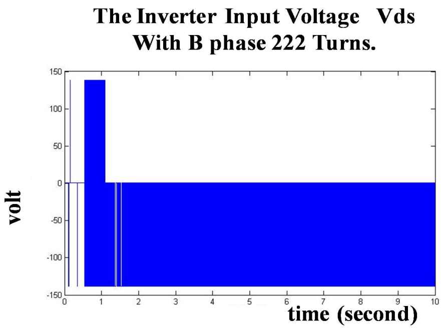

Figure 18: The input inverter voltage-phase B 222 turns

The inverter input voltage shows that the voltage choice from input signal *look up table* to inverter , at time 6.2 seconds until 7.2 seconds the input voltage motor is realize disturbance , the choice process voltage is bad , is shown as figure 19.

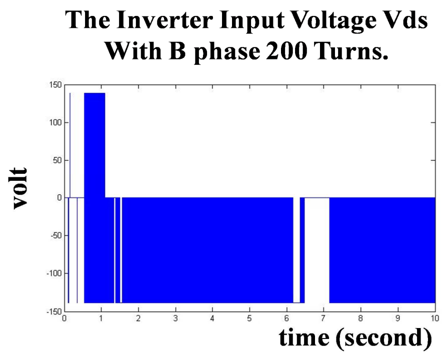

Figure 19: The input inverter voltage-phase B 200 turns

From figure 2 , if the phases current in its lines have disturbance, The influence of the flux to the electromagnetic torque and also the choice of the voltage from look up table under influence of input of the electromagnetic torque and the flux stator , so that the output is the inverter input . As the current phase and the stator flux decrease , that it the input voltage of inverter so very bad, this condition show the short circuit turn-to turn at B phase.

4. CONCLUSION

The rise in disturbance of the motor speed shows, that it conditions is a unbalancing asymetrical turn, that it become the unbalancing motor current, in the line current phase, and this condition is also created due to asymmetrical winding resistances or it shows to indicate the short circuit at this phase . The decreasing disturbance of the stator flux shows, a presented the error of stator flux, if it is compared to the normal stator flux, that it occure

ISSN: 1992-8645 www.jatit.org E-ISSN: 1817-3195

the short circuit turn-to turn at this phase. The strong influence of the flux to the electromagnetic torque, shows the electromagnetic torque disturbance increase, this indicate the short circuit at this phase. The PI Controller gives well result response speed , whice influence of difference resistance, has strong influence to the flux and torque motor. Still bigger and bigger the stator resistance difference with normal condition ,therefore the current at phase defect, overshoot very high and the flux decrease and the inverter input voltage is realize disturbance.. For the future this research can combined using the method of Motor Current Signature Analysis (MCSA) based diagnostics of the stator winding short circuit fault and analysis using Fast Fourier Transform (FFT) for currents phase or Wavelet Transform.

REFERENCE

[1] Wan Shuting, Li Heming , Li Yonggang, Meng Fanchao "Analysis of stator winding parallel-connected branches circulating current and its application in generator fault diagnosis" *Conference: Industry Applications Conference, 2005. Fourtieth IAS Annual Meeting. Conference Record of the 2005, Volume: 1* DOI: 10.1109/IAS.2005.1518289

[2] Li Heming, Wan Shuting, Li Yonggang, Wang Aimeng "Condition monitoring of generator stator winding inter-turn short circuit fault based on electrically excited vibration "*Electric Machines and Drives, 2005 IEEE International Conference on; 06/2005*

[3] Li Yonggang ,Wan Shuting, Li Heming , Zhao Hua . "Fault identification method of rotor inter turn short-circuit using stator winding detection" *Conference: Electrical Machines and Systems, 2003. ICEMS 2003. Sixth International Conference on,* Volume 2 DOI: 10.1109/ICEMS.2003.1274185

[4] C.S. Kallesoe, "Model based stator fault detection in induction motor", *IEEE Annual Ind. Application society meeting, IAS-2008,* pp. 1-8, 2008.

[5]. Wallin, M.. "Measurement and modelling of unbalanced magnetic pull in hydropower Generators." *Digital Comprehensive Summaries of Uppsala Dissertations from the Faculty of Science and Technology 1029. 51 pp. Uppsala.* ISBN 978-91-554-8619-8. 2013.

[6] M. Arkan, "Stator Fault Diagnosis in Induction Motors", *University of Sussex, Ph.D. Thesis*, 2000.

[7] M. Arkan, P.J. Unsworth,"Stator fault diagnosis in induction motors using power decomposition". *in: Phoenix, USA, October, Proceedings of the IEEE Industry Applications Conference 34th Annual Meeting*, 2005, vol. 3, pp. 1908–1912.

[8] Abhisek Ukil, Shuo Chen, Andrea Adenna "Detection of stator short circuit faults in three-phase induction motors using motor current zero crossing instants" *Electric Power Systems Research , Volume 81, Issue 4,* April 2011, Pages 1036–1044

[9] Mirko Cettolo, and Milutin Pavlica "The impact of the induction motor on short-circuit current "..IEEE Industry Applications Magazine July/August 2001

[10] C.H. De Angelo, G.R. Bossio, S.J. Giaccone, M.I. Valla, J.A. Solsona, and G.O. Garcia, "On-line model based stator fault detection and identification in induction motors", *IEEE Trans. On Ind. Elect.,* vol. 56, issue 11, pp.4671-4680, 2009.

[11] D.C. Patel and M.C. Chandorkar, "On-line load test for induction machine stator inter-turn fault detection under stator electrical asymmetries", *Proc. IEEE 36th Annual Conf. on Ind. Elect., IECON-2010,* pp. 933-937, 2010

[12] Yun Jangho, L. Kwanghwan, L. Kwang-woon, L. Bin Sang and YooJi-Yoon, "Detection and classification of stator turn faults and high resistance electrical connections for induction machines", *IEEE Trans. On Ind. Appl.* Vol. 45,issue 2, pp. 666-675, 2009.